SCIENCE CHINA
Information Sciences

• **Supplementary File** •

Ultra-High Gain Hot-Electron Tunneling Transistor Approaching the Collection Limit

Jun LIN[1,2,4*], Pengfei LUO[2,4], Xinpei DUAN[2], Wujun ZHANG[2], Chao MA[2], Tong BU[2], Wanhan SU[2], Bei JIANG[1*], Guoli LI[2], Xuming ZOU[2], Ting YU[3], Lei LIAO[2*] & Xingqiang LIU[2*]

[1]*Faculty of Physics and Electronic Science, Hubei University, Wuhan 430062, China;;*
[2]*State Key Laboratory for Chemo/Biosensing and Chemometrics, College of Semiconductors (College of Integrated Circuits) Hunan University, Changsha 410082, China;;*
[3]*School of Physics and Technology, Wuhan University, Wuhan 430072, China;;*
[4]*J. Lin and P. Luo contribute equally to this work;;*
**Corresponding author (Email: jiangbei@whu.edu.cn, liuxq@hnu.edu.cn, liaolei@whu.edu.cn)*

Appendix A

Figure S1 presents the schematic diagrams of fabrication processes. Briefly, a few-layer MoS_2 flake is mechanically exfoliated by Scotch tape and transferred onto p^+-silicon substrate with 300 nmSiO_2 layer. The contact regions are defined by e-beam lithography (EBL). Then HfS_2 with atomically flat HfO_2 layer is transferred onto MoS_2 flake with physical transfer method, and the HfO_2 TB layer is formed by mild oxidation treatment of HfS_2 in air before transfer process, as shown in Figure S1a. Subsequently, HfO_2 layer that serves as FB layer of HETs formed by the same method, as shown in Figure S1b. Due to the high thermal stability of HfO_2, atomically flat HfO_2 is conformally formed on top of unoxidized HfS_2 through layer-by-layer oxidation and the thickness of HfO_2 layer can be controlled by oxidation temperature and time. Finally, multilayer GeSe with a thickness of $\sim$ 30 nm is transferred to the overlapped region of MoS_2 and HfS_2 by dry transfer process, which can reduce scattering effect from collector, as shown in Figure S1c.

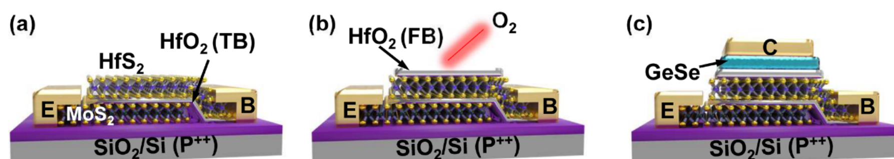

Figure S1 Schematic images of the fabrication processes.

* Corresponding author (email: jiangbei@whu.edu.cn, liuxq@hnu.edu.cn, liaolei@whu.edu.cn)

Appendix B

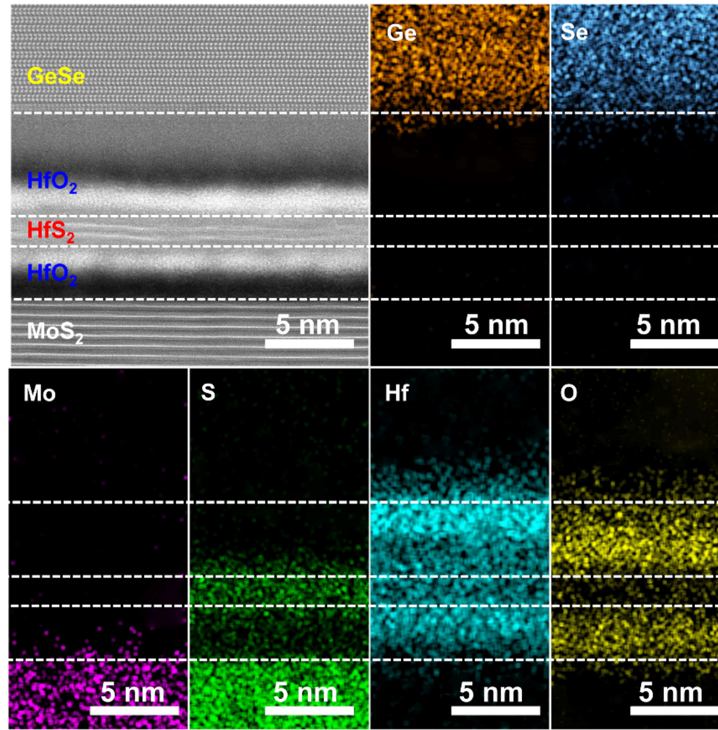

Figure S2 TEM image and elements distribution across the HETs.

Appendix C

Figure *S*3 are output characteristics of the HETs with different original thicknesses of HfS_2 base region. With high $V_{\rm CE}$, barrier height of collector-base junction is reduced, and tunneling hot electrons lead to increment of $J_{\rm C}$. Moreover, a positive $V_{\rm CE}$ enhances electric field generated by $V_{\rm BE}$, capable of continuously lowering tunneling barrier height. Thus, $J_{\rm C}$ is further enhanced. Due to the atomically thickness of HfS_2 base region, hot electrons from emitter can overcome barrier layers and directly contribute to $J_{\rm C}$. As thickness of HfS_2 base region increases, output current is slightly increased, which can be attributed to the reduction of base region resistance. Figure S3a-c are collection efficiency and current gain in common emitter configuration, respectively. Scaling down the thickness of base region below the MFP of hot electron can promote the transition time and weaken the electrostatic decoupling of the collector and emitter. Therefore, reduced HfS_2 base thickness affords large β values, and HETs obtain a record $\beta = 24104$ among the previously reported works. As momentum difference is large when hot electrons pass through 2D/3D interface from 2D to 3D, 2D/2D heterojunctions consisting of atomically flat HfO_2 layers and 2D materials (MoS_2, HfS_2, GeSe) can minimize momentum mismatch, and the rationally designed energy band alignment can reduce back scatter issues in the devices, leading to reduced scattering and reflection events. Moreover, van der Waal heterogeneous integration provides sharp bond-free interfaces with few traps, which accelerates hot electrons tunneling. When hot electrons with sufficient kinetic energy traverse across TB, due to the atomically thickness of HfS_2 base, they are barely consumed and ballistically transport into collector region. However, as the original HfS_2 base is further thinned down to below 10 layers (~ 7.5 nm), the HfS_2 base will be totally oxidized, and negligible current can be detected. Therefore, the current gain maximizes when the base region achieves a critical original thickness of 10 layers.

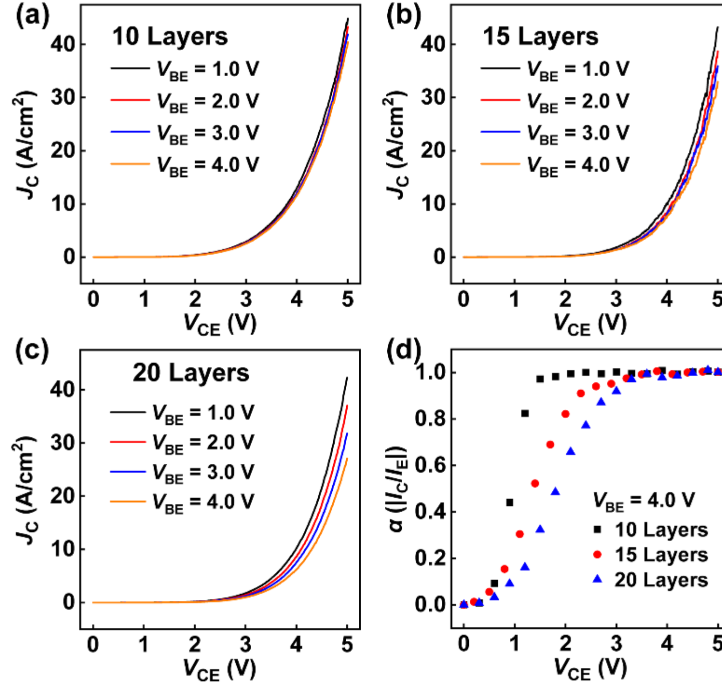

Figure S3 Electrical performance of HETs with common-emitter configuration at room temperature. (a)-(c) Typical output characteristics of the HETs with different original HfS_2 thicknesses. V_{BE} is limited to 4.0 V to avoid electrical breakdown of base-emitter junction. (d) Influence of base-region thickness on α.

Appendix D

Figure S4 shows typical temperature dependent electrical performance of the HETs. Dependence of hot electrons concentration at MoS_2/HfO_2 interface on temperature is reflected by the relationship

$$N_n = c\left(\frac{2\pi m_n kT}{h^2}\right)^{\frac{3}{2}} \exp\left(-\frac{E_F - E_C}{kT}\right) \tag{1}$$

where c, m_n, h, k, T, E_F and E_C are constant, effective mass, Plank constant, Boltzmann constant, thermodynamic temperature, Fermi level and conduction band level, respectively. Fowler- Nordheim tunneling (FNT) current is proportional to hot-electron concentration and increases with temperature increment, and hot-electron kinetic energy increases with ambient temperature, improving injection efficiency of hot electrons across barriers. Therefore, the current density is increased with temperature.

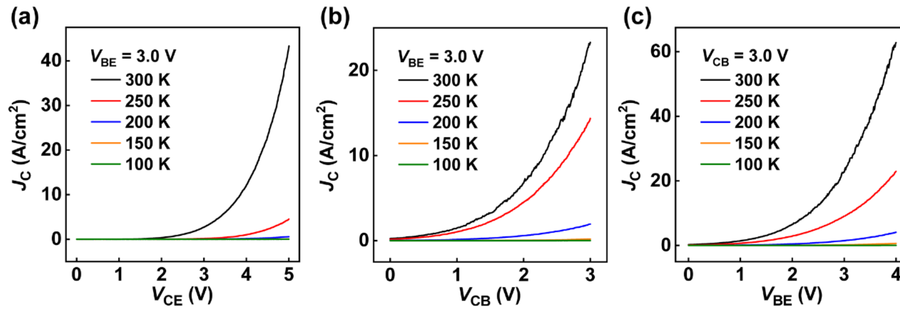

Figure S4 Temperature dependent electrical performance of HETs with common-based configuration. (a)J_C versus V_{CE} characteristics at $V_{BE} = 3$ V. (b)J_C versus V_{CB} characteristics at $V_{BE} = 3$ V. (c)J_C versus V_{BE} characteristics at $V_{CB} = 3$ V.